Chinese Chemical Letters

journal homepage: www. elsevier. com

Communication

A general strategy for selective detection of hypochlorous acid based on triazolopyridine formation

Yanhui Zhang[a,1], Hao Teng[a,1], Ying Gao[a], Muhammad Wasim Afzal[a], Jingye Tian[a], Xi Chen[a], Haoyang Tang[b], Tony D. James[c], Yuan Guo[a,*]

[a] *Key Laboratory of Synthetic and Natural Functional Molecule Chemistry of the Ministry of Education, National Demonstration Center for Experimental Chemistry Education, College of Chemistry and Materials Science, Northwest University, Xi'an 710127, PR China*
[b] *School of Automation, Xi'an University of Posts and Telecommunications, Xi'an, 710121, PR China*
[c] *Department of Chemistry, University of Bath, Bath BA2 7AY, United Kingdom*

ARTICLE INFO

Article history:
Received
Received in revised form
Accepted
Available online

Keywords:
Triazolopyridines
2-Pyridylhydrazones
Fluorescent probes
Reactive oxygen species
Hypochlorous acid

ABSTRACT

Triazolopyridines are an important kind of fused-ring compounds. A HOCl-promoted triazolopyridine formation strategy is reported here for the first time in which hypochlorous acid (HOCl) mildly and efficiently promotes the formation of 1,2,4-triazolo[4,3-α]pyridines **NT1**-**NT6** from various 2-pyridylhydrazones **N1**-**N6**. **N6**, a rhodol-pyridylhydrazone hybrid, was developed into a fluorescent probe for the selective detection of HOCl, and successfully applied to probe endogenous HOCl in living cells and zebrafish *in situ* and in real time. The present intramolecular cyclization reaction is selective and atom-economical, thereby not only providing an important approach for the convenient synthesis of triazolopyridines, but also offering a general strategy for sensitive, selective and biocompatible detection of endogenous HOCl in complex biosystems.

Biological hypochlorous acid (HOCl) is an interesting type of reactive oxygen species (ROS) that plays crucial roles in beneficial immunoregulatory response and pathogenic oxidative stress injuries [1-3]. At the cellular level, HOCl is endogenously generated by a myeloperoxidase (MPO)-catalyzed oxidation reaction between chloride ions (Cl^-) and hydrogen peroxide (H_2O_2) [3-4]. Although HOCl with antimicrobial activity is valuable for host defense during microbial invasion [5], the generation of excessive HOCl leads to many diseases related to oxidative stress damage including aging [6], cancer [7], inflammation [8] and neuro-degenerative disorders [9]. Therefore, highly selective and sensitive tools for the detection of HOCl levels in complex biosystems are of particular interest for accurate clinical diagnosis. For this purpose, methods, including chromatographic, electrochemical, colorimetric and fluorescence, have been developed, among which, nondestructive fluorescence methods based on small-molecule probes are the most desirable for real-time and *in situ* detection [10].

In recent years, a number of small-molecule fluorescent probes have been developed for the detection of HOCl *in vivo* [5,10-23]. Some of them have been designed based on the C=N unit [20-23]. Generally, these types of probes contain acyclic C=N bonds and are non-fluorescent due to isomerization quenching. When HOCl reacts with the C=N, the isomerization is removed, thus leading to a turn-on fluorescence response. According to the reaction mechanism reported in the literature [21], HOCl is able to react with the C=N bond to form formyl or carboxyl compounds *via* hydrolysis and oxidization. Based on this oxidation-leaving group approach, many HOCl probes have been developed [20-21], but significant background interference and lack of selectivity have limited their application in complex biosystems.

The aforementioned concerns encouraged us to develop a powerful new strategy in order to improve the performance of this type of probe. According to a previous report [24], I^+ from the decomposition of I_2 can attack the C=N bond of 2-pyridylhydrazone thereby inducing 2-pyridylhydrazone to form 1,2,4-triazolo[4,3-α]pyridine through a cyclization reaction (Scheme 1a). We speculated that HOCl containing a positive monovalent chlorine should also be able to convert 2-pyridylhydrazone into 1,2,4-triazolo[4,3-α]pyridine. To prove

* Corresponding author.
E-mail address: guoyuan@nwu.edu.cn (Y. Guo).
[1] These authors contributed equally to this work.

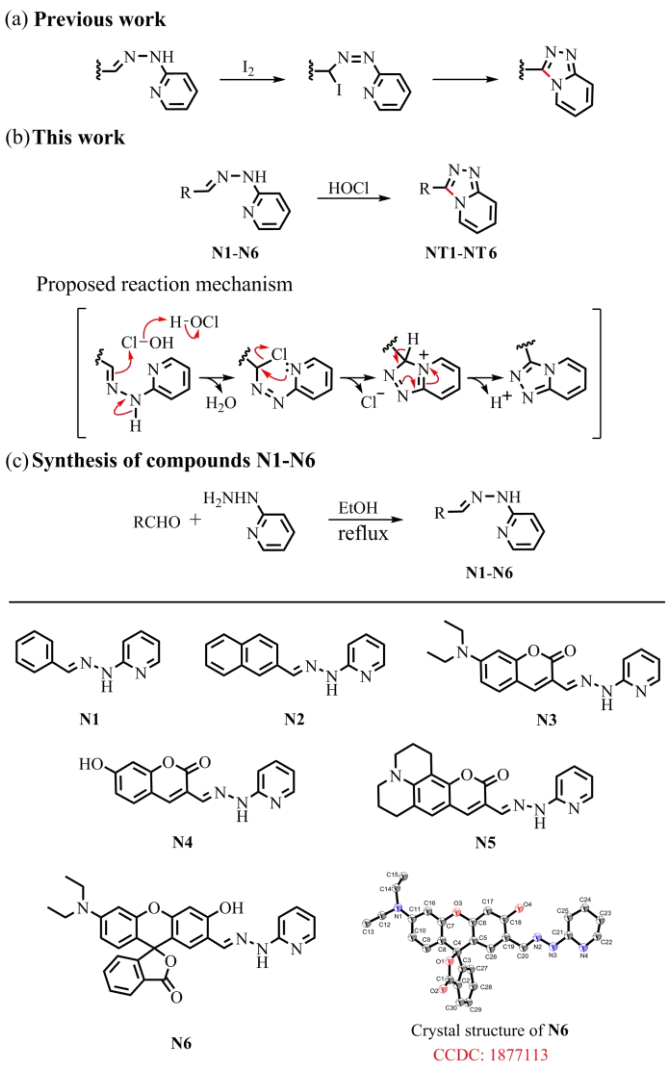

Scheme 1. (a) Previous work. I_2-promoted triazolopyridine formation strategy. (b) This work. Our new HOCl-promoted triazolopyridine formation strategy. (c) Synthetic route for compounds **N1**-**N6**.

our hypothesis, we synthesized compounds **N1**-**N2** by the reaction of 2-hydrazinopyridine with benzaldehyde or naphthaldehyde. As show in Fig. S1a and S1b (in Supporting information), the spectra signals of **N1** and **N2** displayed noticeable changes after the addition of HOCl. Compounds **N1** and **N2** were converted into triazole derivatives (**NT1**-**NT2**) after being treated with HOCl, which were validated by HRMS (Fig. S2 and S3 in Supporting information). In light of these encouraging results, we further synthesized compounds **N3**-**N6** (potential HOCl probes) through the condensation of 2-hydrazinopyridine and diverse aldehyde fluorophores, including coumarin (**N3**-**N5**) and xanthene (**N6**) scaffolds. Furthermore, we obtained the crystal structure of compound **N6** (Table S1 in Supporting information). Detailed experimental procedures and characterization of compounds **N1**-**N6** and compounds **NT1**-**NT6** can be found in the supporting information. The spectral properties of **N3**-**N6** before and after the addition of HOCl were investigated in a physiological buffer solution (Fig. S1c-1f in Supporting information). As expected, HRMS results show that compounds **N3**-**N6** were also converted into the corresponding triazole derivatives (**NT3**-**NT6**) after treatment with HOCl (Fig. S4-S7 in Supporting information). Moreover, taking the **N6** as an example, we measured the spectra of **NT6** and the reaction product of **N6** with HOCl. The emission and absorption wavelengths of **NT6** are consistent with that of **N6** treated with HOCl, demonstrating that **NT6** was the product of **N6** with HOCl (Fig. S8 in Supporting information). In accordance with the optical spectrum, ^{1}H NMR characterization data indicate that the reaction of **N6** with HOCl results in the disappearance of the signal at 11.16 ppm (=N-NH- proton of **N6**), and the ^{1}H NMR spectrum is well matched with that of **NT6** (Fig. S9 in Supporting information). Taken together, all these results further support our hypothesis that the sensing event proceeds through HOCl-promoted triazolopyridine formation.

A plausible reaction mechanism for HOCl-promoted triazolopyridine formation is shown in Scheme 1b. Taking the formation of **N6** as an example, chlorination occurs on the C=N bond of **N6** using Cl^+ from HOCl. Then, the chloro-substituted carbon atom is then attacked by the pyridine nitrogen to produce the 3*H*-1,2,4-triazolo[4,3-α]pyridin-4-ium intermediate through a 5-*exo-tet* cyclization, in which a new C-N bond is formed. Finally, the triazolopyridine framework is formed by deprotonation and rearomatization.

Among the compounds we designed, **N6** is the most promising compound for detecting HOCl. After treatment with HOCl, **N6** was transformed into triazolopyridine derivative **NT6** (Fig. 1a), resulting in the generation of an intense golden fluorescence and 159-fold enhancement in fluorescence intensity. The pK_{cycl} value of **N6** was calculated to be 4.43 (Fig. S10a in Supporting information), meaning that **N6** was mainly present in the unconjugated spirolactone form without fluorescence at pH 7.4. The C=N isomerization-induced fluorescence quenching is the other reason why **N6** is not fluorescent causing negligible background fluorescence. On the other hand, the pK_{cycl} of **NT6** was calculated to be 8.98 (Fig. S10b in Supporting information), indicating that **NT6** would mainly exist in the ring-opened π-conjugated form with strong fluorescence at pH 7.4. Therefore, the **N6** displayed a rapid response (45 s), high selectivity towards HOCl over other ROS and RNS as well as sensitive detection of

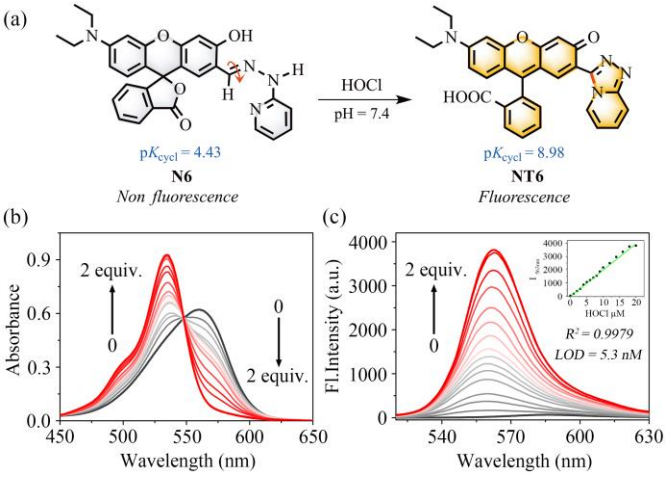

Fig. 1. (a) Recognition strategy of **N6** towards HOCl. (b) UV-vis absorption spectra of **N6** (10 μM) upon treatment with HOCl (0-2 equiv.) in pH 7.4 PBS buffer solution. (c) Fluorescence emission spectra changes of **N6** (10 μM) upon treatment with HOCl (0-2 equiv.) in pH 7.4 PBS buffer solution. Inset: Linear correlation of **N6** towards the concentrations of HOCl. λ_{ex} = 505 nm, λ_{em} = 563 nm, slit: 2.5 nm/5 nm.

HOCl with a detection limit of 5.3 nM. Remarkably, **N6** was successfully used to visualize HOCl in living cells and zebrafish.

The pH-dependent fluorescence changes of **N6** towards HOCl were then evaluated. Fig. S11 (in Supporting information) shows that **N6** was very stabled and was able to respond to HOCl over a broad pH range from 5.5 to 11.0. In order to facilitate biological applications, a pH of 7.4 was selected for examining the spectral properties of probe **N6**. Therefore, we titrated HOCl with probe **N6** in PBS buffer solution (pH = 7.4) and the process was monitored by UV-vis absorption. As shown in Fig. 1b, the maximum absorption peak of probe **N6** (10 μM) was at 562 nm (ε = 61900 $M^{-1}\cdot cm^{-1}$). However, with successive additions of HOCl (0-2.0 equiv.) to the solution of **N6**, the absorption peak at 562 nm reduced gradually and synchronously a new absorption peak emerged at 534 nm (ε = 92600 $M^{-1}\cdot cm^{-1}$) with an isosbestic point at 548 nm. These results indicated the formation of a new product after the addition of HOCl into a solution of **N6**. Fluorescence titrations were then conducted in PBS buffer solution (pH = 7.4) (Fig. 1c). **N6** (Φ_f = 0.01) had minimal fluorescence, while the addition of HOCl into the **N6** solution led to a 159-fold increase in fluorescence intensity at 563 nm, which was interpreted as the formation of **NT6** (Φ_f = 0.30). Moreover, the fluorescence intensity at 563nm displayed an excellent linear relationship (R^2 = 0.9979) with HOCl concentrations ranging from 0 to 18 μM. The detection limit of **N6** for HOCl was calculated to be 5.3 nM (Fig. 1c). All these results clearly indicate that **N6** can detect HOCl quantitatively.

The time-dependence of the fluorescence intensity at 563 nm of probe **N6** in the absence and presence of HOCl was also evaluated. As shown in Fig. S12 (in Supporting information), with the addition of HOCl to a solution of **N6**, the fluorescence intensity at 563 nm gradually enhanced with increasing reaction time and reached a plateau within 45 s. The reaction rate of probe **N6** with HOCl is very fast, which is crucial for real-time detection of HOCl *in vivo*.

To assess the selectivity of **N6** towards HOCl, we investigated the fluorescence spectra of probe **N6** towards various reactive nitrogen species (RNS), reactive oxygen species (ROS), common anions and biothiols. As shown in Fig. 2a, the fluorescence intensity at 563 nm was enhanced remarkably after the addition of HOCl, with an obvious fluorescence change (Fig. 2a inset),

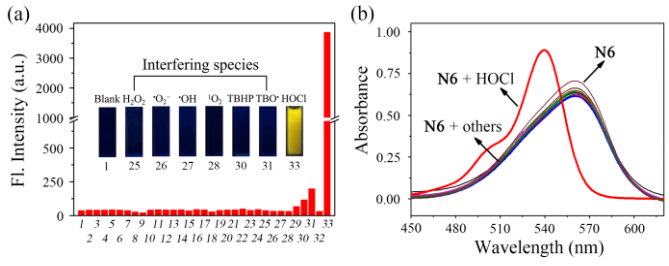

Fig. 2. (a) Fluorescent response of **N6** (10 μM) in the presence of various analytes (2 equiv.) in PBS buffer solution (20 mM, pH = 7.4, containing 20% EtOH). Inset: visual fluorescence color under a handheld 365 nm UV lamp. (b) UV-vis absorbance spectra of probe **N6** (10 μM) in the presence of various analytes (2 equiv.) in PBS buffer solution (20 mM, containing 20% EtOH). (1: Blank, 2: HS^-, 3: F^-, 4: Cl^-, 5: Br^-, 6: I^-, 7: $S_2O_3^{2-}$, 8: AcO^-, 9: SO_4^{2-}, 10: NO_2^-, 11: NO_3^-, 12: CN^-, 13: SCN^-, 14: PO_4^{3-}, 15: $H_2PO_4^-$, 16: HPO_4^{2-}, 17: HCO_3^-, 18: HSO_4^-, 19: HSO_3^-, 20: SO_3^{2-}, 21: CO_3^{2-}, 22: Cys, 23: Hcy, 24: GSH, 25: H_2O_2, 26: $^{\bullet}O_2^-$, 27: $^{\bullet}OH$, 28: $^1O_2$, 29: $NO^{\bullet}$, 30: TBHP, 31: $TBO^{\bullet}$, 32: $ONOO^-$, 33: HOCl), λ_{ex} = 505 nm, λ_{em} = 563 nm, slit: 2.5 nm/5 nm.

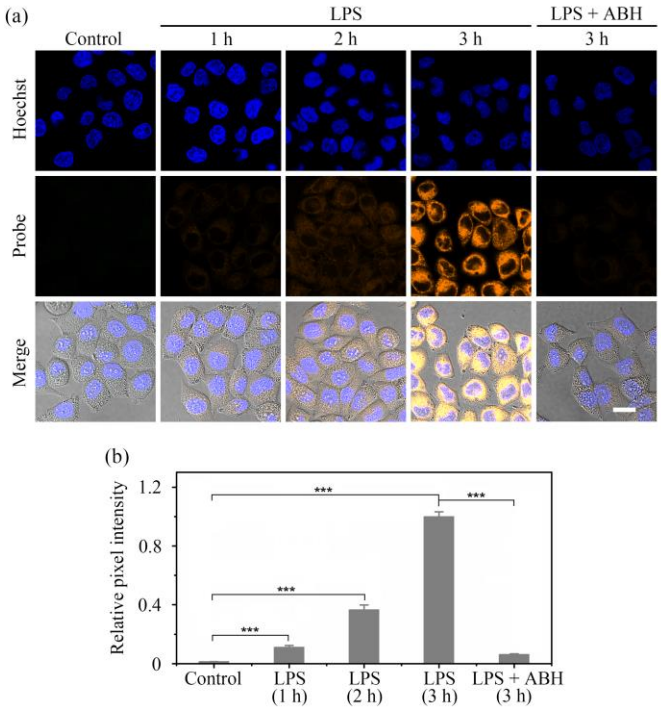

Fig. 3. (a) Confocal fluorescent images of **N6** in HepG2 cells under different conditions. HepG2 cells pretreated with LPS for 0 h (first column), 1 h (second column), 2 h (third column) and 3 h (fourth column), and then stained with **N6** (5 μM, 5 min) and Hoechst (10 μg/mL, 20 min); Cells (fifth column) were stimulated with LPS (5 μg/ml) and ABH (250 μM) for 3 h, and then incubated with **N6** (5 μM, 5 min) and Hoechst (10 μg/mL, 20 min). (b) Normalized intensity of the fluorescence images of (a). The results are presented as the mean ± SD (n = 3). ***p < 0.001, two-sided Student's *t*-test. (Hoechst, λ_{ex} = 405 nm, λ_{em} = 425-475 nm; Probe, λ_{ex} = 488 nm, λ_{em} = 500-550 nm; scale bar = 20 μm).

while other biologically relevant substances did not trigger any significant changes under similar conditions. Simultaneously, we investigated the absorption spectra of **N6** towards various analytes. In Fig. 2b, only HOCl caused a distinct change of the absorption spectra, whereas other analytes gave rise to negligible changes. In addition, a competitive binding assay was performed by adding HOCl to the mixed solution of **N6** and other species (Fig. S13 in Supporting information). The competitive experiments indicate that other analytes did not interfere with the detection of HOCl by **N6**. These results clearly indicate that **N6** has excellent selectivity for HOCl over other analytes and can be used for the accurate detection of HOCl in complex systems.

Inspired by the excellent sensing performance of **N6** towards HOCl *in vitro*, we postulated that **N6** could be used for imaging HOCl in living cells. Prior to cellular imaging tests, the cytotoxicity of **N6** was evaluated using a methyl thiazolyl tetrazolium (MTT) assay in HepG2 cells. It was clear from those tests that probe **N6** has low cytotoxicity. (Fig. S14 in Supporting information). Therefore, probe **N6** was used to detect the level of exogenous HOCl in HepG2 cells. As shown in Fig. S15 (in Supporting information), cells incubated with only probe **N6** were almost non-fluorescent. After these cells were treated with 1 μM, 5 μM and 10 μM HOCl, distinct fluorescence was observed in the yellow channel and the fluorescence intensity of the cells enhanced following the increase of HOCl concentration. Meanwhile, we also explored the ability of **N6** to visualize endogenous HOCl by Bacterial endotoxin lipopolysaccharide (LPS) in HepG2 cells. LPS can stimulate cells to release ROS,

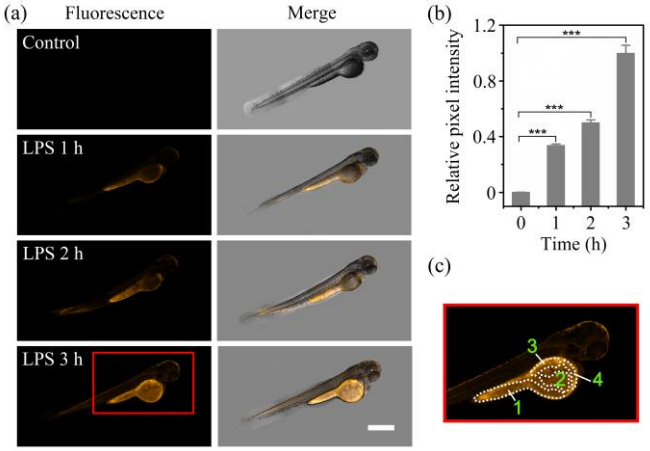

Fig. 4. (a) Representative images from the four groups of zebrafish. Zebrafish pretreated with LPS for 0 h, 1 h, 2 h and 3 h (from top to bottom), and then stained with **N6**. (b) Normalized intensity of the fluorescence images of (a). The results are presented as the mean ± SD (n = 3). ***p < 0.001, two-sided Student's *t*-test. (c) Zoom image of the area indicated with red square (regions: 1, yolk; 2, intestine; 3, kidney; 4, liver). λ_{ex} = 488 nm, λ_{em} = 500-550 nm, scale bar = 500 μm.

such as HOCl [16]. As shown in Fig. 3, no fluorescence was observed in HepG2 cells incubated with only probe **N6**. When **N6**-stained cells were incubated with LPS, the fluorescence signal in the yellow channel became brighter with increasing incubation time from 0 to 3 h. In contrast, 4-aminobenzoic hydrazide (ABH), a well-known MPO inhibitor, can reduce the concentration of endogenous HOCl [15]. As expected, the intracellular fluorescence intensity is clearly decreased in the presence of ABH. These results indicate that probe **N6** is cell membrane permeable and capable of imaging exogenous and endogenous HOCl in living cells without interference from background signals.

Encouraged by the results for cell imaging, we explored the capability of **N6** to image HOCl in zebrafish. As shown in Fig. S16 (in Supporting information), zebrafish incubated with **N6** (50 μM) for 30 min displayed low fluorescence in the yellow channel. Then zebrafish stained by **N6** were incubated with different amounts of HOCl (0, 10, 50 and 100 μM) for 30 min and significant yellow fluorescence was observed. To assess the performance of **N6** in imaging the endogenous HOCl in zebrafish, we further pre-incubated zebrafish with LPS and then with probe **N6**. As shown in Fig. 4, the fluorescence intensity of the zebrafish stimulated by LPS exhibited a time-dependent increase with prolonging the incubation time (0-3 h) and we observed that the endogenous HOCl induced by LPS is mainly accumulated in yolk, intestine, kidney and liver of zebrafish (Fig. 4c). Hence, these results indicate that probe **N6** can detect exogenous and endogenous HOCl *in vivo*.

In conclusion, we report on a new strategy in which a 2-pyridylhydrazone moiety is selectively oxidized by HOCl to 1,2,4-triazolo[4,3-α]pyridine. Featured by mild reaction conditions, triazolopyridines **NT1**-**NT6** have been efficiently synthesized from various 2-pyridylhydrazones. We introduce 2-pyridylhydrazone as a new recognition receptor for HOCl and in particular **N6** with a rhodol skeleton, has been developed as a highly selective fluorescent probe for the detection of HOCl *in vitro* and *in vivo*. This probe displayed a 159-fold rapid (45 s) fluorescence turn-on response with low limit of detection (5.3 nM) for HOCl. Furthermore, probe **N6** was used to image HOCl in living cells and zebrafish respectively with promising results, clearly demonstrating its effectiveness in biological systems. Our present HOCl detection system based on HOCl-promoted triazolopyridine formation is unique and offers a general strategy to design new HOCl fluorescent probes.

Acknowledgments

We gratefully acknowledge the financial support from National Natural Science Foundation of China (21977082, 21472148 and 21807088), Open Funding Project of the State Key Laboratory of Bioreactor Engineering (2018OPEN12), Special Foundation of the Education Committee of Shaanxi Province (18JK0702), Technology Plan Project of Xi'an [201805040YD18CG24(1) and GXYD18.1] and Academic Backbone of Northwest University Outstanding Youth Support Program. T.D.J. wishes to thank the Royal Society for a Wolfson Research Merit Award.

Appendix A. Supplementary data

Supplementary data associated with this article can be found, in the online version, at

References

[1] J. Zielonka, J. Joseph, A.Sikora, et al., Chem. Rev. 117 (2017) 10043-10120.
[2] T. Nybo, S. Dieterich, L.F. Gamon, et al., Redox Biol. 20 (2019) 496-513.
[3] T.H.D. Araujo, S.S. Okada, E.E.B. Ghosn, et al., Cell. Immunol. 281 (2013) 27-30.
[4] L. Wu, I.C. Wu, C.C. DuFort, et al., J. Am. Chem. Soc. 139 (2017) 6911-6918.
[5] Z. Mao, M. Ye, W. Hu, et al., Chem. Sci. 9 (2018) 6035-6040.
[6] J. Luo, K. Mills, S.L. Cessie, R. Noordam, D.V. Heemst, Ageing Res. Rev. 57 (2020) 100982.
[7] D. I. Pattison, M. J. Davies, Biochemistry, 45 (2006) 8152-8162.
[8] J. Kay, E. Thadhani, L. Samson, B. Engelward， DNA Repair 83 (2019) 102673.
[9] P. Palladino, F. Torrini, S. Scarano, M. Minunni, J. Pharmaceut. Biomed. 179 (2020) 113016.
[10] D. Shi, S. Chen, B. Dong, et al., Chem. Sci. 10 (2019) 3715-3722.
[11] H. Xiong, L. He, Y. Zhang, et al., Chin. Chem. Lett. 30 (2019) 1075-1077.
[12] Y. Chen, T. Wei, Z. Zhang, et al., Chin. Chem. Lett. 28 (2017) 1957-1960.
[13] J. Lv, F. Wang, T. Wei, X. Chen, Ind. Eng. Chem. Res. 56 (2017) 3757-3764.
[14] Y.L. Pak, S.J. Park, G. Song, et al., Anal. Chem. 90 (2018) 12937-12943.
[15] P. Wei, L. Liu, Y. Wen, et al., Angew. Chem. Int. Ed. 58 (2019) 4547-4551.
[16] X. Zhang, W. Zhao, B. Li, et al., Chem. Sci. 9 (2018) 8207-8212.
[17] X. Chen, F. Wang, J.Y. Hyun, et al., Chem. Soc. Rev. 45 (2016) 2976-3016.
[18] Y.L. Pak, S.J. Park, D. Wu, et al., Angew. Chem. Int. Ed. 57 (2018) 1567-1571.
[19] J. Lv, Y. Chen, F. Wang, et al., Dyes Pigm. 148 (2018) 353-358.
[20] X. Cheng, H. Jia, T. Long, et al., Chem. Commun. 47 (2011) 11978-11980.
[21] B. Wang, D. Chen, S. Kambam, et al., Dyes Pigm. 120 (2015) 22-29.
[22] W.L. Wu, Z.M. Zhao, X. Dai, L. Su, B.X. Zhao, Sens. Actuators B 232 (2016) 390-395.
[23] Y. Zhang, L. Ma, C. Tang, et al., J. Mater. Chem. B 6 (2018) 725-731.
[24] E. Li, Z. Hu, L. Song, W. Yu, J. Chang, Chem. Eur. J. 22 (2016) 11022-11027.